Materials Science and Engineering B 180 (2014) 27–32

Contents lists available at ScienceDirect

Materials Science and Engineering B

journal homepage: www.elsevier.com/locate/mseb

Analysis of impurities with inhomogeneous distribution in multicrystalline solar cell silicon by glow discharge mass spectrometry

C. Modanese*, L. Arnberg, M. Di Sabatino

Department of Materials Science and Engineering, Norwegian University of Science and Technology (NTNU), Alfred Getz vei 2B, N-7491 Trondheim, Norway

ARTICLE INFO

Article history:
Received 3 May 2013
Received in revised form 9 October 2013
Accepted 23 October 2013
Available online 6 November 2013

Keywords:
Glow discharge mass spectrometry (GDMS)
Trace elements
Multicrystalline silicon
Extended defects
Bulk analysis

ABSTRACT

Multicrystalline silicon for solar cells presents material inhomogeneities related to the presence of extended defects such as grain boundaries or dislocations. These defects are possible sources for nucleation of precipitates, which generally show a highly inhomogeneous distribution in the crystal structure. The use of direct current (dc), continuous operation glow discharge mass spectrometry (GDMS) as an analytical technique to study these distributions is presented in this article, with focus on ultra-trace elements such as Fe and Cu. In order to evaluate the impact of the analytical parameters, a doping element (B) is also analyzed, since it generally shows a more homogeneous distribution in the crystal structure. The results suggest that, for commonly used mc-Si for solar cells, due to the size of the precipitates and the high degree of inhomogeneity in the bulk, single precipitates cannot be detected during common bulk analysis by dc GDMS.

1. Introduction

The performance of multicrystalline silicon solar cells is ultimately limited by carrier recombination in the substrate, which is dominated in practice by recombination related to impurities, decorated dislocations and grain boundaries [1]. Average metals concentrations of 1 ppma (5×10^{16} cm^{-3}) have been shown to lead to nanometer-scale precipitates/agglomerates, which are present on μm-scale areas, especially at dislocations, and at a lower extent at grain boundaries and microdefects [2]. Metal silicide precipitates have been observed in TEM studies on as-grown mc-Si, with sizes from tens of nanometers to several hundreds of nanometers in large multi-metal clusters [3,4]. In those studies, Fe, Ni and Cu were found to be present; and many of the precipitates were nucleated around dislocations or grain boundaries. Stokkan *et al.* [5] modeled and evaluated experimentally the combined effect of grain boundaries and dislocations on minority carrier lifetime, showing that recombination activity of grain boundaries can be related to their misorientation. Since the concentration of metal impurities in the silicon substrate [1] and their spatial distribution (*i.e.*, precipitated at grain boundaries or dislocations, or dissolved into the Si lattice) plays a major role on the performance of the solar cell device, studying the distribution of impurities in the bulk of mc-Si materials is the aim of the present work.

In the last decades, glow discharge mass spectrometry (GDMS) has become a well-established technique for multi-element investigation of trace- and ultra-trace impurities in highly pure metals and semiconductors [6]. Details on the technique can be found in Ref. [7]. With focus on PV materials, GDMS is widely used in the industry for the chemical analysis of upgraded metallurgical grade and solar grade silicon feedstock thanks to the low detection limits achievable (potentially down to pptw) [8]. Moreover, contrarily to most of the other techniques employed to measure the chemical composition of Si feedstock, sample preparation for GDMS does not require any sample dissolution, which in itself can introduce external contamination [9]. A further advantage of GDMS is the possibility for depth profiling of multi-layered structures over a relatively large bulk area [9]. GDMS analyses are carried out on areas typically 50 mm^2, which can provide a rather representative value of the bulk concentration/distribution of the impurities. Since the calibration for each element has a weak dependence on the sputtering rate of the matrix composition, quantitative multi-elemental analysis can be carried out directly [10]. The precision of the quantitative measurements of Si feedstock had been quantified to be ±10–25%, increasing with decreasing concentration of the impurity [8]. Note that, since materials with high enough conductivity are needed in order to establish a stable glow discharge, analyses on electronic grade materials are extremely challenging, particularly at low doping levels.

* Corresponding author. Tel.: +47 41520593.
E-mail address: chiara@material.ntnu.no (C. Modanese).

0921-5107/$ – see front matter © 2013 Elsevier B.V. All rights reserved.
http://dx.doi.org/10.1016/j.mseb.2013.10.010

Depth profiling by GDMS is usually performed using standard bulk methods to determine the analytical concentration [11]. A few studies of depth profiling of crystalline Si are available in the literature, and they have been performed by radio frequency GDMS [9], or by direct current (dc) GDMS [10]. Both studies used pulsed sources, whose advantage over continuous operation is related to an enhanced sputter atom yield (*i.e.*, ionization rate/count rate), and to an increased signal-to-noise ratio due to greater excitation and ionization [12]. However, continuous, dc-powered GDMS sources are currently more widely used and well-established quantification procedures are readily available. Moreover, Schmitt *et al.* [10] observed a rather high detection limit of 100 ppbw for P due to a loss in sensitivity in the pulsed-operated dc-GDMS. Those studies focused on B and P, elements that are most likely neither segregating at grain boundaries nor precipitating in mc-Si materials. It is worth noting that, in order to obtain a low detection limit and hence a high sensitivity in the analysis, GDMS calibration should aim for a high sputtering rate, possibly coupled with high integration times. However, this affects in turn the depth resolution of the analyses since the mass spectrometer operates in scanning mode [10]. In addition, the impact on depth resolution becomes more relevant in the case of a multi-elemental analysis.

Dc high resolution (HR) GDMS analyses were tuned in the present study with the aim of investigating the extent of impurities inhomogeneity in mc-Si materials for PV applications, *e.g.*, the presence of precipitates. Two types of impurities are analyzed, namely i) metal impurities (Fe and Cu) and ii) doping element (B). The impurities are selected with the twofold aim of being representative of elements usually present in the Si for solar cells, and providing an understanding of the spatial distribution of elements that are likely precipitating (metal impurities), and elements that are generally homogeneously distributed into the Si matrix (doping elements). Depth profiles of the impurities concentrations are taken for this purpose, with focus on the relation to crystal structure on one side, and to the homogeneity of the distribution on the other side. The number of analyzed impurities is limited in order to obtain a high depth resolution. Both the expected concentration of impurities and the expected size of precipitates are used to tune the analysis parameters.

2. Experimental

In this work, samples from two directionally solidified mc-Si ingots are analyzed by a HR-GDMS, Element GD instrument from Thermo Scientific. A first ingot, named S2, was selected in order to investigate the presence of precipitates and the homogeneity of the spatial distribution of impurities, with particular focus on the effect of (random) grain boundaries. Ingot S2 is a representative of solar grade silicon materials for solar cells. The samples are taken high in the ingot, *i.e.*, close to the end of the solidification, where a higher concentration of impurities is expected due to segregation during solidification. A second ingot, named D6, was selected to focus on the distribution and segregation of Fe. Ingot D6 is a standard p-type mc-Si material, but with 50 ppmw Fe added to the melt. The samples are reported according to their height along the ingot (solid fraction). All samples are cut perpendicularly to the ingot growth direction, *i.e.*, the sputtering direction is parallel to the growth direction. The samples are ground on SiC papers. The sputtered area is about 8 mm in diameter. Electron backscatter diffraction (EBSD) maps are taken for the samples from ingot S2 in order to confirm the grain orientations of the spots analyzed by GDMS. In particular, twin boundaries Σ3, Σ9 and Σ27 are highlighted.

The dc-GDMS parameters are kept as similar as possible between the various samples. The discharge current is similar for all the samples, whereas the discharge Ar gas flow is 300 ml/min and 400 ml/min for samples from ingot S2 and D6, respectively. GDMS is a comparative technique [13], where quantification of the impurities is performed through internal standards, considering the total ion current and the impurity ion current. In the present work, the quantification is performed manually, integrating the peak intensity and subtracting the background intensity for each isotope. This allows having better control over the background noise on the observed peaks, particularly relevant for analyses with very low counts. The quantification of the impurity concentration is obtained from the ion beam ratio (IBR) and the relative sensitivity factor (RSF):

$$C_x = IBR_x \cdot x \cdot RSF_x = (I_x/Ab_x)/(I_m/Ab_m) \cdot x \cdot RSF_x \quad (1)$$

where I is the intensity [counts per second (CPS)] and Ab is the abundance of the (impurity) isotope x and the matrix isotope m. The RSF takes into account the analytical sensitivity for different elements; consequently, it is matrix- and element specific. The formula is valid for low concentrations, characteristic of impurities in silicon for solar cells. The procedure followed to calculate the RSFs can be found in Ref. [14]. Two different sets of RSFs are used for the ingots S2 and D6, since the discharge gas has a strong influence on the factor. For the analyses reported in this work, the detection limit is ~1.5 ppbw for both Fe and Cu.

Table 1
Parameters of the methods used for the analyses. Total time includes the processing time required by the software.

Ingot	Method	Analysis time (s)				
		^{11}B	^{56}Fe	^{63}Cu	^{28}Si	Total
S2	–	20	20	20	5	66
D6	#1	–	25	–	6	33
D6	#2	25	–	–	6	33
D6	#3	25	25	–	6	58

The analysis times for each isotope are reported in Table 1. The time for each isotope is set considering the expected concentration and the targeted depth resolution in the analysis. The total time is the time for one repetition, *i.e.*, a complete analysis of the isotopes included in the list. The sputtering rate for the analysis parameters used here is approximately 1 μm/min, which corresponds to ~0.1 mg Si/μm sputtered. The analyses are carried out in a sequential order on the same crater, i.e., the depth of the sputtered material increases with increasing the repetition number.

3. Results

Three different areas, namely i) single grain, ii) with random grain boundaries, and iii) with twin boundaries, were visually selected on a slice from ingot S2. These are named SG1, GB1 and TW1, respectively. EBSD maps were collected on the three spots after GDMS analysis (Fig. 1). The inverse pole figure shows the color code for the grain orientations, where the z-direction is the ingot growth direction. The white dots in the maps are non-indexed points. The highlighted grain boundaries are Σ3, Σ9 and Σ27, and the non-colored grain boundaries in GB1 map are random grain boundaries. It can be observed that SG1 does not have any grain boundaries. GB1 presents some twin boundaries (of these, most are Σ3), together with other random grain boundaries; whereas TW1 has only twin boundaries, the vast majority being Σ3.

The concentrations of B, Fe and Cu in samples from ingot S2 are reported in Fig. 2. 'Repetition #' in the x-axis refers to a complete analysis, *i.e.*, B, Fe and Cu measured in sequence. The spots labeled 're-ground' are on the same position as before grinding, *e.g.*, SG1 re-ground is taken right below the SG1 spot. The re-grinding was aimed at studying possible macrosegregation in the samples. Only three repetitions are taken for SG1, GB1 and TW1 spots; and they are reported as repetitions #16–18 to take into account the

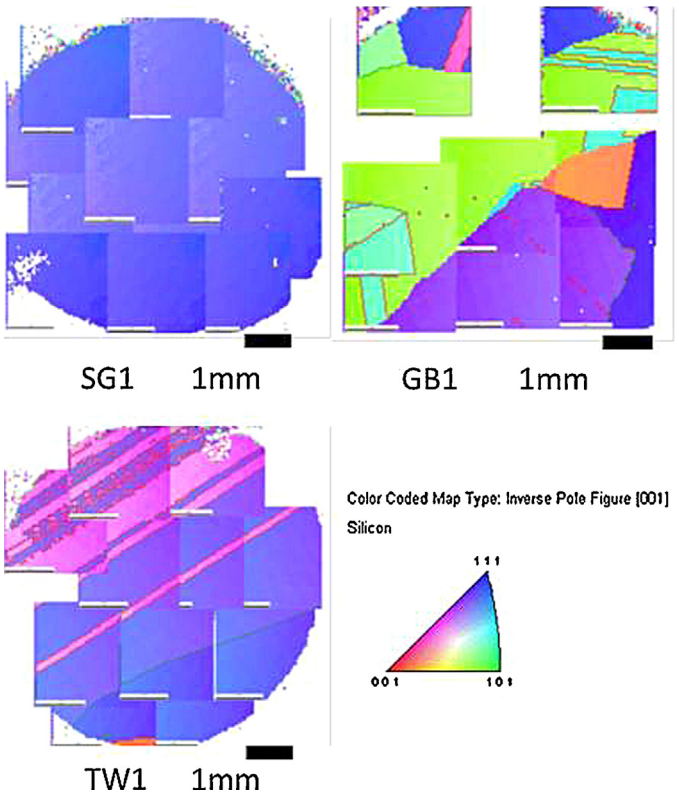

Fig. 1. EBSD maps of the spots SG1, GB1 and TW1 from ingot S2 after the first GDMS measurement. The highlighted grain boundaries are Σ3 (red), Σ9 (green) and Σ27 (violet) boundaries. The color scale in the inverse pole figure is valid for all the maps.

10 min pre-sputtering, which is not adopted for the analyses on the re-ground spots. Note that, since the analysis times for each repetition are different for the first series compared with the re-ground series, 'repetition #' on the *x*-axis cannot be translated into sputtering depth in a straightforward manner. SG1 area shows an unexpectedly higher concentration of B compared with both GB1 and TW1. Neither the Fe nor the Cu concentrations show any clear differences between the three types of spots. Nevertheless, SG1 re-ground and TW1 re-ground show Fe peaks close to the end of the analyses. An apparent higher Cu concentration is observed for the first few repetitions in GB1 re-ground.

The average concentrations and the relative standard deviations of the analyses shown in Fig. 2 are reported in Table 2. For the spots analyzed after re-grinding, the values are calculated both for all the repetitions, and for the repetitions after the commonly used sputtering time (*i.e.*, 10 min). No significant variation is observed for Fe or Cu in any spot, except for GB1 re-ground. The relative scatter is greater for Fe and Cu than for B, whereas the absolute standard deviation is lower.

The GDMS analyses on samples from ingot D6 are reported in Figs. 3–5. A comparison of the profiles for Fe (spot #1) and B (spot #2) shows a higher relative scatter in the Fe concentrations, although the absolute variation is lower. A third series of measurements (spot #3) was carried out with a concurrent analysis of B and Fe (Fig. 5), and a similar trend in the scatter among the repetitions is observed. As for the analyses on the other ingot, 'repetition #' on the *x*-axis cannot be directly translated into a depth of sputtering axis, due to the different analysis times among the spots. The total analysis time, and consequently the total sputtered depth, are similar for all the spots. Apparent higher concentrations of both B and Fe are measured in sample 84% for the first 10 repetitions.

The lower scatter in the Fe concentration profiles compared with B is confirmed in the standard deviations for the various spots. A

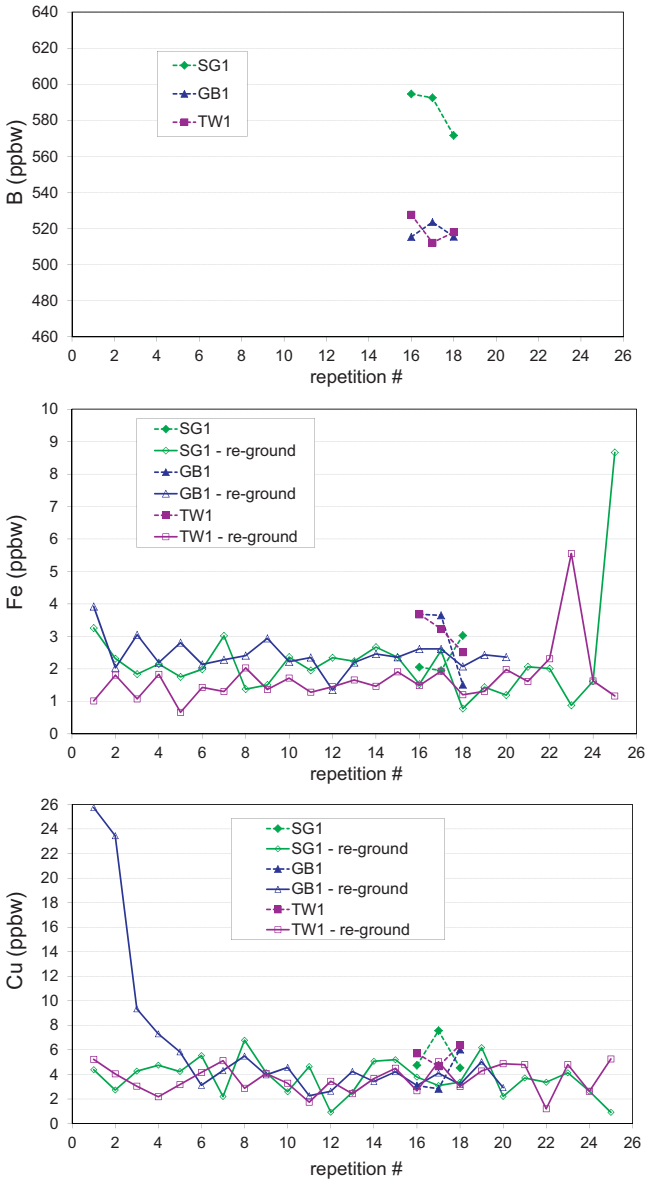

Fig. 2. B (top), Fe (center) and Cu (bottom) concentrations measured in SG1, GB1 and TW1 spots from ingot S2. 'Re-ground' refers to a second grinding of the sample. 'Repetition #' refers to an analysis of all the three impurities.

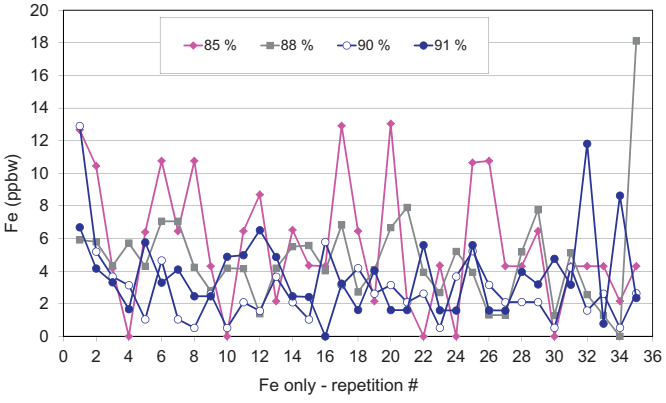

Fig. 3. Fe concentration analyzed in spot #1 in samples from ingot D6. The samples are labeled according to the height along the ingot.

Table 2
Average values and relative standard deviations for the analyses on the spots from ingot S2.

Spot	Repetitions included	B			Fe			Cu		
		Average ppbw		RSD %	Average ppbw		RSD %	Average ppbw		RSD %
SG1	16–18	586.2	±	1.8%	2.3	±	21%	5.6	±	25%
GB1	16–18	518.2	±	0.7%	3.0	±	34%	4.0	±	36%
TW1	16–18	519.3	±	1.2%	3.1	±	15%	5.6	±	13%
SG1 re-ground	1–25		–		2.2	±	66%	3.7	±	39%
SG1 re-ground, w/o presputt	14–25		–		2.3	±	90%	3.6	±	39%
GB1 re-ground	1–20		–		2.4	±	21%	6.4	±	101%
GB1 re-ground, w/o presputt	14–20		–		2.4	±	8%	3.7	±	21%
TW1 re-ground	1–25		–		1.7	±	52%	3.7	±	32%
TW1 re-ground, w/o presputt	14–25		–		1.9	±	58%	3.9	±	32%

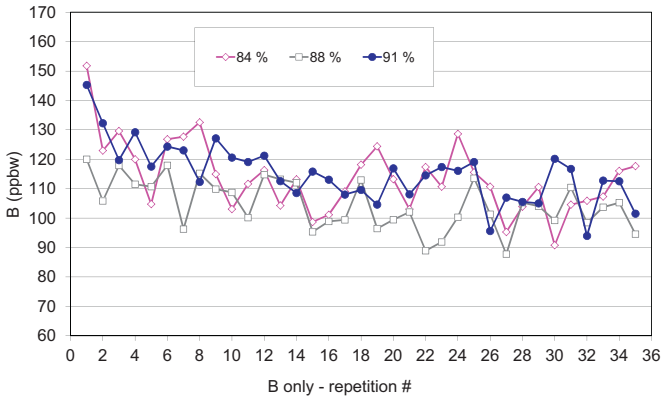

Fig. 4. B concentration analyzed in spot #2 in samples from ingot D6. The samples are labeled according to the height along the ingot.

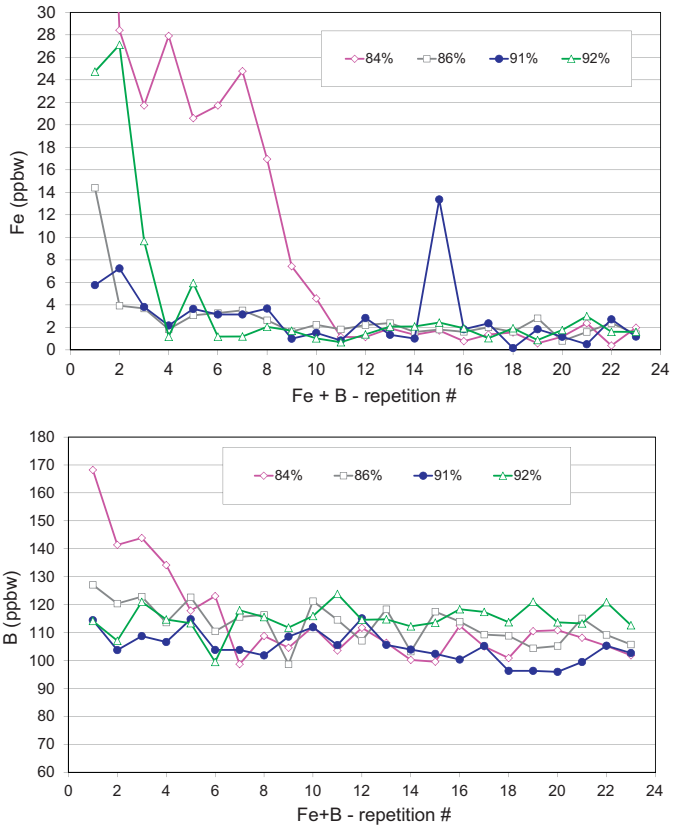

Fig. 5. Fe (top) and B (bottom) concentrations measured in the same spot, spot #3, of the samples from ingot D6. 'Repetition #' refers to the analysis of both B and Fe. The samples are labeled according to the height along the ingot.

greater relative standard deviation is observed for Fe compared with B (Table 3), although the absolute values are lower for Fe. Note that all the repetitions are included in the calculations.

The depth profile of the crater of the GDMS measurements was measured by white light interferometer on the crater of sample D6 – spot#2 – 84%. Two line scans were collected, and the resulting average depth is ∼20 μm, with minimum and maximum in the crater of 15 μm and 27 μm, respectively. The profile confirms that the average sputtering rate is ∼1 μm/min. The topography of the crater is not axial-symmetrical.

4. Discussion

4.1. Optimization of analytical parameters

The integration time for each isotope (Table 1) is selected as a compromise between the expected concentrations, *i.e.*, high

Table 3
Average values and relative standard deviations for the analyses on the spots from ingot D6.

Sample	Spot	Repetitions included	B			Fe		
			Average ppbw		RSD %	Average ppbw		RSD %
84%	Spot#2	1–35	113.8	±	10%		–	
84%	Spot#3	1–23	114.3	±	15%	11.7	±	147%
85%	Spot#1	1–35		–		5.6	±	69%
86%	Spot#3	1–23	113.1	±	6%	2.8	±	93%
88%	Spot#1	1–35		–		4.7	±	65%
88%	Spot#2	1–35	104.7	±	8%		–	
90%	Spot#1	1–35		–		2.9	±	78%
91%	Spot#1	1–35		–		3.7	±	64%
91%	Spot#2	1–35	115.0	±	9%		–	
91%	Spot#3	1–23	104.9	±	5%	2.9	±	96%
92%	Spot#3	1–23	114.8	±	4%	4.3	±	163%

enough to have few counts, and the expected size of precipitates, *i.e.*, low enough to obtain one or more repetitions within a single precipitate. Our experience with previous analyses of similar materials was used as guideline, and suggested not to decrease the integration time further. Given the sputtering rate of 1 μm/min, each repetition for each impurity isotope corresponds to ∼0.3 μm for analyses on S2 samples, and ∼0.4 μm for analyses on D6 samples. Considering this sputtered depth and assuming that a precipitate i) consists only of one element (*e.g.*, Fe) and ii) is perfectly spherical, calculations show that in order to detect 5 ppbw of the element, the precipitate must have a diameter in the range ∼0.5–2 μm. Several studies have observed multi-metal precipitates or clusters of several hundreds micrometers in mc-Si for solar cells [2–4], and they have been found to be dispersed over μm-scale regions [15]. Hence, the applied analysis parameters should have allowed for single, large precipitates to be sputtered and analysed in the depth profile.

It could be argued that when carrying out the depth profiling presented here, an important aspect to evaluate is the shape of the sputtered crater. The profile of the crater bottom measured by white light interferometer is non-axial-symmetrical, thus showing a non-atomically flat sputtering. This clearly reduces the depth resolution of the analysis, which is intended as the capability of the technique to distinguish between two consecutive layers in a layered structure [13]. Nevertheless, the effect of the non-flatness of the bottom is greatly limited by short analyses and a high number of repetitions. Moreover, as discussed later, inhomogeneity in the distribution of impurities in the mc-Si bulk renders the flatness of the crater bottom irrelevant.

The analyses on samples from ingot S2 and D6 have different sets of discharge gas flow. Although this parameter strongly affects both the RSFs and the sputtered depth, it results in no significant difference in the analyses performed. Similar detection limits and concentration trends are observed for the same isotope along the depth-axis.

All the analyses, excluding the ones on SG1, TB1 and TW1, are carried out without the usual 10 min pre-sputter, although ∼30 s of sputtering are used to perform the tuning of the discharge parameters for each analysis. Plasma stabilization times are generally in the order of tens of minutes for metallic samples analyzed by dc-GDMS [16], and in order to shorten them a sacrificial mc-Si blank sample is analyzed prior to each sample. This pre-cleaning of the anode surface ensures the reduction of the effect of plasma instabilities on the first repetitions during the analyses [9]. Moreover, it also reduces any effect of external contamination, *e.g.*, contaminants present on the anode's inner surface from previous analyses. Hence, the concentration profiles presented here show much shorter plasma stabilization times, usually 1–2 min, *i.e.*, within repetition #2–4. These results suggest that surface analysis of solar grade crystalline Si materials is possible with dedicated tuning of the discharge and careful sample surface cleaning.

To summarize, the parameters that were found to be optimal for the instrument used in this work, to carry out depth profile analysis of silicon materials for PV, are i) integration time of ∼20 s/impurity, ii) discharge gas flow of 300–400 ml/min, and iii) source cleaning with a blank silicon sample to reduce the plasma stabilization time.

The average matrix intensities and their relative standard deviations are valuable to assess the impact of plasma stabilization times on the analyses. The average intensities are in the range 1.1×10^{10}–2.3×10^{10} and 1.0×10^{9}–1.1×10^{10} cps for samples from ingot S2 and D6, respectively. The standard deviations are in the range 0.8–6.2% for ingot S2, and in the range 0.6–6.4% and 0.5–4.1% for ingot D6 including all repetitions and after ∼10 min sputtering, respectively. The standard deviations tend to be slightly higher when considering all the repetitions, which is due to a slow decrease of the matrix intensity over time, in turn related to the deepening of the crater. Nevertheless, the variation among consecutive repetitions is limited, and consequently has a negligible effect on the quantification of the impurities, which is done on the basis of a single repetition. Moreover, the low deviations in the matrix intensities over time lead to stable and uniform conditions for the quantification of impurities, thus increasing the precision.

Depth profiles obtained on SiC materials showed that the use of a μs-pulsed source increases the depth resolution compared with the continuous operation mode for the same GD equipment [17]. The use of a μs-pulsed source for mc-Si materials could thus favor the analysis of precipitates by decreasing the sputtered depth between consecutive repetitions, whilst maintaining a high sensitivity. However, Schmitt *et al.* [10] have observed a strong increase in the detection limit for a μs-pulsed source on crystalline silicon materials compared with a continuous source.

4.2. Material-related inhomogeneity

The concept of representative sampling [8] has to be considered when discussing the impact of material inhomogeneity on the GDMS analysis. The occurrence of precipitates in the matrix is highly irregular, especially in materials with low concentration of impurities as those analyzed in this study. Metal-based precipitates have been observed to occur on a μm-scale in mc-Si materials with ∼1 ppma of impurities [2], *i.e.*, three orders of magnitude higher than the levels present in our materials. Therefore, these materials might have precipitates distributed on a much coarser scale compared with the sputtering depth of any GDMS analysis, and are therefore not detected in the analyses presented here.

The capability of the technique used in this work to detect precipitates in mc-Si was shown by Ryningen *et al.* [18]. In the study, clusters of Ca-containing precipitates, several millimeters in length and 200–300 μm in width, were analyzed and compared with cluster-free areas from the same ingot. The analyses on the precipitate-rich areas quantified the Ca concentration in the order of several hundreds ppbw, measured with ∼1 μm resolution over a total sputtered depth of ∼15 μm; whereas the analyses on the precipitate-free areas showed Ca levels below the detection limit (*i.e.*, Below ∼50 ppbw).

The analyses on samples from ingot S2 (Fig. 2) show no significant variation in the Fe and Cu concentration. This is partly unexpected, considering that segregation of metal impurities is highly unlikely in regions with no grain boundaries and low dislocation density, *i.e.*, SG1 and TW1 regions. As mentioned above, the spatial distribution of precipitates could account for this. Moreover, the sputtered area in the analyses is ∼50 mm^2, and the fraction of this area covered by grain boundaries is limited (*i.e.*, the average grain size is in the order of few millimeters). This decreases the probability of sputtering a precipitate on a grain boundary during the analysis. The apparent higher Cu concentration for the first few repetitions in GB1 re-ground sample is most likely related to surface effect.

The concentration of B analyzed in SG1 area is much higher than in TW1 and GB1 areas. Resistivity measurements in these materials showed stable values, and such a localized microsegregation of the B distribution is rare to observe. However, this is clearly a material property and not a measurement artifact. The concentration of B in SG1 is ∼20% higher than in GB1 and TW1, where an accuracy of ±10% is expected for these analyses [14]. Although highly unlikely, macrosegregation of boron in mc-Si cannot be completely excluded, and these results show that minor inhomogeneities are present in the material.

The analyses show a greater absolute scatter for B than for Fe and Cu, both when the impurities are measured on different areas and on the same area, *i.e.*, where the effect of macrosegregation in the material is greatly reduced. It is worth noting that GDMS

analyses generally have a concentration-dependent accuracy [8], *i.e.*, lower concentrations lead to lower accuracy. However, these results suggest that impurities with very low concentrations (Fe and Cu) can be measured with at least the same accuracy as impurities with concentration 1–2 orders of magnitude higher (B). These results indicate the advantage of the GDMS technique for the quantification of ultra-trace elements. On the other hand, they also underline that several repetitions are needed in order to obtain an accurate average concentration both for doping elements and for metallic impurities in mc-Si. This is an important aspect to consider during routine analysis of impurities concentration in the bulk.

The analysis on the sample from ingot D6 – spot #3 – 84% seems to differ from the others, with a much higher concentration of both Fe and B measured during the first 10 repetitions. Although all samples were prepared following the same procedure, it is not clear whether this profile is due to a thicker native oxide layer on the surface [9], or if it is representative of a true concentration. The stability in the intensity of the plasma from the very first repetition suggests the second is more likely.

5. Conclusion

In this study we have presented depth profile analyses of mc-Si for solar cells performed with dc, HR-GDMS operated in continuous mode. These materials are known to be inhomogeneous, and the GDMS analyses are aimed at studying their inhomogeneity.

The results show that impurities present in the low-ppb level (*e.g.*, transition metals) have lower variation in the quantified concentration than impurities present in concentrations 1–2 orders of magnitude higher (*e.g.*, boron). These impurities can be measured with high repeatability. This aspect is of particular relevance for the PV industry to evaluate the number of repetitions necessary for accurate routine analyses. On the other hand, no significant difference in their distribution was observed when analyzing different grains of the materials.

This study suggests that, although mc-Si materials are known to be inhomogeneous and to lead to microsegregation of impurities at low-energy sites as grain boundaries, two factors practically hinder the possibility of investigation of inhomogeneity and precipitates distribution by dc-HR, continuous operation mode GDMS. Firstly, GDMS is a scanning technique and its depth resolution has a similar or higher order of magnitude compared with the expected size of precipitates. Secondly, the spatial distribution of precipitates is highly irregular, and the probability of their occurrence within the sputtered volume is rather small.

Acknowledgment

The authors would like to thank the 'Norwegian Research Centre for Solar Cell Technology' (project number 193829), a Centre for Environment-friendly Energy Research co-sponsored by the Norwegian Research Council and research and industry partners in Norway. Special thanks to Torild Krogstad (NTNU) for assistance in the lab; to Joachim Hinrichs (ThermoScientific) for discussion; and to Børge Holme (SINTEF) for the depth profile.

References

[1] G. Coletti, Prog. Photovolt. Res. Appl. 21 (2012) 1163–1170.
[2] S. McHugo, A.C. Thompson, I. Perichaud, S. Martinuzzi, Appl. Phys. Lett. 72 (1998) 3482–3484.
[3] H. Nordmark, M. Di Sabatino, M. Acciarri, J. Libal, S. Binetti, E.J. Øvrelid, J.C. Walmsley, R. Holmestad, EBIC, EBSD and TEM study of grain boundaries in multicrystalline silicon cast from metallurgical feedstock, in: 33rd IEEE Photovoltaic Specialists Conference, San Diego, CA, 2008.
[4] H. Nordmark, Microstructure studies of silicon for solar cells, PhD thesis, Faculty of Natural Sciences and Engineering, Norwegian University of Science and Technology, 2009.
[5] G. Stokkan, S. Riepe, O. Lohne, W. Warta, J. Appl. Phys. 101 (2007) 053515.
[6] C. Venzago, M. Weigert, Fresenius J. Anal. Chem. 350 (1994) 303–309.
[7] R.K. Marcus, J.A.C. Broekaert (Eds.), Glow Discharge Plasmas in Analytical Spectroscopy, John Wiley & Sons, Chichester, 2003, pp. 71–96.
[8] R. Hockett, Advanced analytical techniques for solar-grade feedstock, in: S. Pizzini (Ed.), Advanced Silicon Materials for Photovoltaic Applications, John Wiley & Sons, Chichester, 2012, pp. 215–234.
[9] J. Pisonero, L. Lobo, N. Bordel, A. Tempez, A. Bensaoula, N. Badi, A. Sanz-Medel, Solar Energy Mater. Solar Cells 94 (2010) 1352–1357.
[10] S. Schmitt, C. Venzago, B. Hoffmann, V. Sivakov, T. Hofmann, J. Michler, S. Christiansen, G. Gamez, Prog. Photovol. Res. Appl. (2012), http://dx.doi.org/10.1002/pip.2264.
[11] A. Bengston, Depth profile analysis, in: Glow Discharge Plasmas in Analytical Spectroscopy, John Wiley & Sons, Chichester, 2003, pp. 141–154.
[12] W.W. Harrison, C. Yang, E. Oxley, Mass spectrometry of glow discharges, in: Glow Discharge Plasmas in Analytical Spectroscopy, John Wiley & Sons, Chichester, 2003, pp. 71–96.
[13] T. Nelis, J. Pallosi, Appl. Spectrosc. Rev. 41 (2006) 227–258.
[14] M. Di Sabatino, A.L. Dons, J. Hinrichs, L. Arnberg, Spectrochim. Acta B Atom. Spectrosc. 66 (2011) 144–148.
[15] S. McHugo, Appl. Phys. Lett. 71 (1997) 1984–1986.
[16] R.K. Marcus, Radio frequency glow discharges, in: Glow Discharge Plasmas in Analytical Spectroscopy, John Wiley & Sons, Chichester, 2003, pp. 97–140.
[17] G. Churchill, K. Putyera, V. Weinstein, X. Wang, E.B.M. Steers, J. Anal. Atom. Spectrom. 26 (2011) 2263–2273.
[18] B. Ryningen, T. Ervik, E. Olsen, E. Øvrelid, G. Stokkan, M. Kivambe, C. Modanese, O. Lohne, On the role of calcium in multicrystalline silicon, in: Proceedings of the 27th European Photovoltaic Solar Energy Conference, Frankfurt, Germany, 2012.